PROCEEDINGS OF SCIENCE

Charged particle correlations with ATLAS

Róbert Astaloš[a,*] **on behalf of the ATLAS Collaboration**

[a] *Comenius University,*
Šafárikovo námestie 6, Bratislava, Slovakia

E-mail: robert.astalos@cern.ch

Correlations between charged particles provide an important insight about hadronization processes. Results on Bose-Einstein two-particle correlations (BEC) using ATLAS data from LHC proton-proton collisions at the center-of-mass energy of 13 TeV are presented. Data were collected in a special low-luminosity configuration with a minimum-bias trigger and a high-multiplicity track trigger, accumulating integrated luminosities of 151 μb^{-1} and 8.4 nb^{-1}, respectively. The BEC are measured for pairs of like-sign charged particles, each with $|\eta| < 2.5$ and for two kinematic ranges: $p_{\mathrm{T}} > 100$ MeV and $p_{\mathrm{T}} > 500$ MeV. The BEC parameters, characterizing the source radius and particle correlation strength, are investigated as functions of charged-particle multiplicity (up to 300) and average transverse momentum of the pair (up to 1.5 GeV). The double-differential dependence on charged-particle multiplicity and average transverse momentum of the pair is also studied. The BEC radius is found to be independent of the charged-particle multiplicity for high multiplicity (above 100), confirming a previous observation at lower energy. This saturation occurs independently of the transverse momentum of the pair.

41st International Conference on High Energy physics - ICHEP2022
6-13 July, 2022
Bologna, Italy

*Speaker

PoS(ICHEP2022)802

1. Introduction

Particle correlations play an important role in the understanding of multiparticle production in hadron–hadron, hadron–nucleus and nucleus–nucleus collisions. Correlations between two identical bosons, called Bose–Einstein correlations, (BEC), are a well known phenomenon in high-energy and nuclear physics. The BEC are often considered to be the analogue of the Hanbury Brown and Twiss effect [1] in astronomy, describing the interference of incoherently emitted identical bosons [2]. The BEC constitute a sensitive probe of the space-time geometry of the hadronization region, and allow the determination of the size and shape of the source from which particles are emitted.

In this contribution, studies of the BEC in proton-proton collisions at $\sqrt{s}$ = 13 TeV [3] using the ATLAS detector [4] are presented. The same methodology is used as was used in the previous ATLAS BEC studies [5], and the same minimum-bias (MB) trigger is used as was used in an earlier study of charged-particle distributions at 13 TeV [6]. In addition, the study is extended to the region of high-multiplicity collisions by using the high-multiplicity track (HMT) trigger previously used for studies of long-range elliptic azimuthal anisotropies [7]. The MB and HMT datasets were taken in a special configuration of the LHC in June 2015, with low beam currents and reduced beam focusing, producing a low mean number of interactions per bunch-crossing, $\langle\mu\rangle$: in the range 0.003–0.007 for MB events and 0.01–0.04 for HMT events. Selected events correspond to integrated luminosities of 151 μb^{-1} and 8.4 nb^{-1} for the MB and HMT triggers, respectively.

2. Analysis method

The BEC are observed at small values of the size of the four-momentum difference, $Q = \sqrt{|Q^2|}$, between two identical bosons, where $Q^2 = -(p_1-p_2)^2 = M_{12}^2-4m^2$, p_1 and p_2 are the four-momenta of the particles, M_{12}^2 is the invariant mass of the particle pair and m is the particle mass. The BEC parameters are measured in terms of a two-particle correlation function, $C_2(Q) = \frac{\rho(Q)}{\rho_0(Q)} = \frac{\rho(++,--)}{\rho(+,-)}$, where $\rho(Q)$ is the distribution of Q formed from all like-sign charged-particle pairs ($\rho(++,--)$), assuming in this analysis that all charged particles are pions, and $\rho_0(Q)$ is a reference distribution specially constructed to exclude the effect of BEC. In this analysis, $\rho_0(Q)$ is constructed from unlike-sign charged-particle pairs ($\rho(+,-)$). The distributions $\rho(Q)$ and $\rho_0(Q)$ are normalized to unity, i.e. they are probability density functions. To account for the effects of resonances, the $C_2(Q)$ correlation function is corrected by dividing by the corresponding quantity constructed from MC simulations that contain resonances but not the BEC: $R_2 = \frac{C_2^{\rm data}}{C_2^{\rm MC}} = \frac{\rho^{\rm data}(++,--)/\rho^{\rm data}(+-)}{\rho^{\rm MC}(++,--)/\rho^{\rm MC}(+-)}$, where $C_2^{\rm data}(Q)$ and $C_2^{\rm MC}(Q)$ are the $C_2(Q)$ functions reconstructed from data and MC samples, respectively.

The plane wave approch assuming symmetrical two-particle (boson) wave function and spherically symmetrical Cauchy-Lorentz source emission probability distribution described by a single width parameter R referred to as hadronization source radius leads to the following form of the $R_2(Q)$ (as well as $C_2(Q)$) function:

$$R_2(Q) = C_0[1 + \lambda e^{-RQ}](1 + \varepsilon Q), \tag{1}$$

where C_0 is a constant depending on the normalizations of signal and reference distributions, ε describes possible long-distance correlations that have not been removed fully by reference distribution and λ is the correlation strength called also incoherence or chaoticity parameter [8]. In a simplified scheme for fully coherent emission of identical bosons, $\lambda = 0$, while for incoherent (chaotic) emission, $\lambda = 1$. Parameters R and λ are of interest and are extracted from a fit to the $R_2(Q)$ function and studied as functions of track multiplicity and pair transverse momentum. In addition, two possible selections on the p_{T} threshold of the final-state particles are compared.

3. Multiplicity dependence of the fit parameters

The dependence of R and λ parameters on multiplicity is studied in multiplicity intervals that are chosen to be well populated, and comparable to those used by other LHC experiments [9]. To compare the BEC parameters from different p_{T}-thresholds, a scaled charged-particle multiplicity is introduced (multiplicity divided by average charged-particle multiplicity per unit of pseudorapidity in the region $|\eta| < 0.2$ for given cuts and collision energy): $\mathrm{m_{ch}} \equiv \mathrm{n_{ch}}/(5 \times \langle \mathrm{dn_{ch}}/\mathrm{d}\eta|_{|\eta|<0.2} \rangle)$. At 13 TeV, the average charged-particle multiplicity calculated this way is 32.5 for particles with $p_{\mathrm{T}} > 100$ MeV [10] and 16.2 for particles with $p_{\mathrm{T}} > 500$ MeV [6].

The extracted BEC parameters R and λ from fit by Eq. 1 are shown as functions of scaled multiplicity in Figure 1 for $p_{\mathrm{T}} > 100$ MeV and $p_{\mathrm{T}} > 500$ MeV. The MB and HMT data agree well where they overlap.

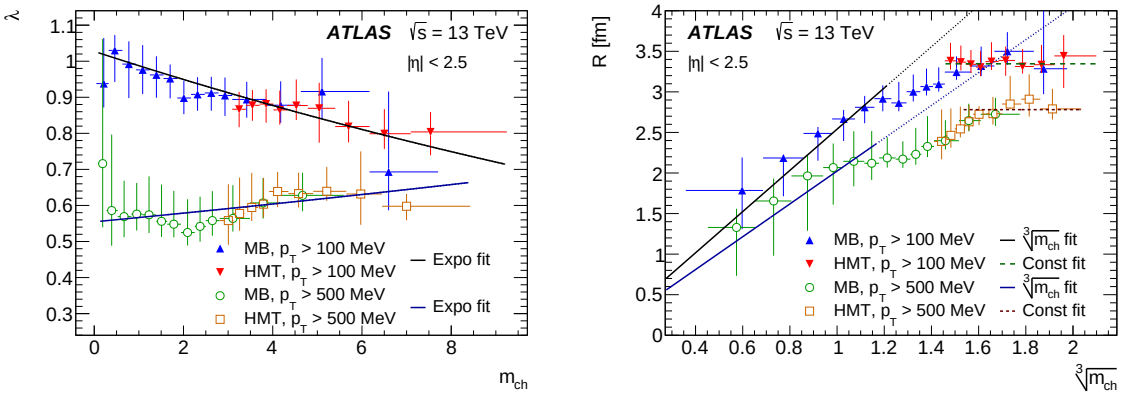

Figure 1: The dependence of the correlation strength, λ, on rescaled multiplicity, $\mathrm{m_{ch}}$, obtained from the fit of the $R_2(Q)$ correlation functions by Eq. 1 for tracks with $p_{\mathrm{T}} > 100$ MeV and $p_{\mathrm{T}} > 500$ MeV at $\sqrt{s}$ =13 TeV for the minimum-bias (MB) and high multiplicity track (HMT) data (left) and the dependence of the source radius, R, on $\sqrt[3]{\mathrm{m_{ch}}}$ (right). The uncertainties represent the sum in quadrature of the statistical and asymmetric systematic contributions. The black and blue solid curves in (left) represent the exponential fit of $\lambda(\mathrm{m_{ch}})$ for $p_{\mathrm{T}} > 100$ MeV and $p_{\mathrm{T}} > 500$ MeV, respectively. The black and blue solid curves in (right) represent the linear fit of $R(\mathrm{m_{ch}})$ for $\sqrt[3]{\mathrm{m_{ch}}} < 1.2$ for $p_{\mathrm{T}} > 100$ MeV and $p_{\mathrm{T}} > 500$ MeV, respectively. The black and blue dotted curves are extensions of the black and blue solid curves beyond $\sqrt[3]{\mathrm{m_{ch}}} > 1.2$, respectively. The green and brown dashed curves represent the saturation value of $R(\mathrm{m_{ch}})$ for $\sqrt[3]{\mathrm{m_{ch}}} > 1.45$ with $p_{\mathrm{T}} > 100$ MeV and for $\sqrt[3]{\mathrm{m_{ch}}} > 1.55$ with $p_{\mathrm{T}} > 500$ MeV, respectively [3].

For $p_{\mathrm{T}} > 100$ MeV, λ decreases with $\mathrm{m_{ch}}$, and the dependence is well described by an exponential decrease. For $p_{\mathrm{T}} > 500$ MeV λ shows only a weak dependence on multiplicity. It is constant within

measurement uncertainties. The different behavior for two p_{T} cuts is explained in Section 5.

The R parameter increases with multiplicity up to about $\mathrm{m_{ch}} \cong 3.08$. For $\mathrm{m_{ch}} \leq 1.7$, R rises with $\sqrt[3]{\mathrm{m_{ch}}}$ linearly. A linear increase of R with $\sqrt[3]{\mathrm{m_{ch}}}$ follows naturally if the hadronization volume is proportional to the number of produced particles. For higher multiplicities, the measured R parameter is observed to be independent of multiplicity. This saturation of the BEC R parameter at high multiplicity is similar to that observed by ATLAS at $\sqrt{s}$ =7 TeV [5] and by CMS at $\sqrt{s}$ =13 TeV [9]. The R dependence shows similar behavior for both p_{T} thresholds. There is a linear rise with $\sqrt[3]{\mathrm{m_{ch}}}$ up to 1.2, after which there is some tapering off towards a plateau for $\sqrt[3]{\mathrm{m_{ch}}} > 1.45$ at $R = 3.35^{+0.20}_{-0.09}$ fm for $p_{\mathrm{T}} > 100$ MeV, and for $\sqrt[3]{\mathrm{m_{ch}}} > 1.6$ at $R = 2.78^{+0.23}_{-0.09}$ fm for $p_{\mathrm{T}} > 500$ MeV.

4. Dependence on the pair average transverse momentum

The average transverse momentum of the pair is defined as: $k_{\mathrm{T}} = |\mathbf{p}_{\mathrm{T},1} + \mathbf{p}_{\mathrm{T},2}|/2$, where $\mathbf{p}_{\mathrm{T},1}$, $\mathbf{p}_{\mathrm{T},2}$ are transverse momenta of two particles in a pair. The BEC are studied in k_{T} intervals from 0.1 to 1.5 GeV that are chosen so that they are populated roughly equally. The dependencies of $R(\mathrm{m_{ch}})$ and $\lambda(\mathrm{m_{ch}})$ for the two p_{T} thresholds are shown in Figure 2. In the small-Q, BEC-sensitive region, the minimum k_{T} is highly correlated with the p_{T} threshold, therefore k_{T} thresholds of 100 MeV and 500 MeV are applied for the p_{T} thresholds of 100 MeV and 500 MeV, respectively. The values of R and λ decrease with k_{T}. The decrease can be described by an exponential function.

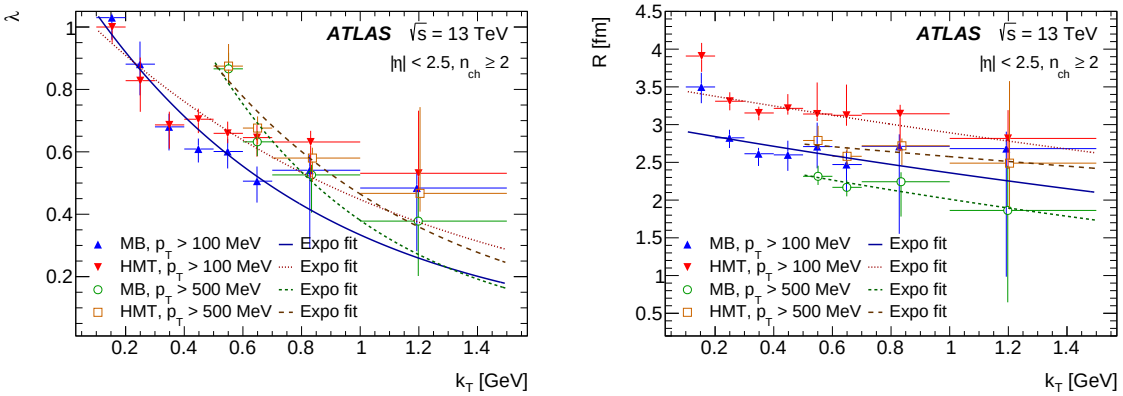

Figure 2: The k_{T} dependence of the correlation strength, λ (left), and the source radius, R (right), obtained from the fit to the $R_2(Q)$ correlation functions by Eq. 1 for events with multiplicity $\mathrm{n_{ch}} \geq 2$ and transverse momentum of tracks with $p_{\mathrm{T}} > 100$ MeV and $p_{\mathrm{T}} > 500$ MeV at $\sqrt{s}$ =13 TeV for the minimum-bias (MB) and high-multiplicity track (HMT) events. The uncertainties represent the sum in quadrature of the statistical and systematic contributions. The curves represent exponential fits [3].

5. Double-differential dependence on $\mathrm{m_{ch}}$ and k_{T}

There is sufficient data at 13 TeV to study the double-differential dependencies: $\lambda(\mathrm{m_{ch}}, k_{\mathrm{T}})$ and $R(\mathrm{m_{ch}}, k_{\mathrm{T}})$. The two-dimensional (2D) dependencies of λ and R for $p_{\mathrm{T}} > 100$ MeV are shown in Figure 3. In order to convey a clear picture of the 2D dependence, the values are presented without uncertainties, but those are generally less than 10%.

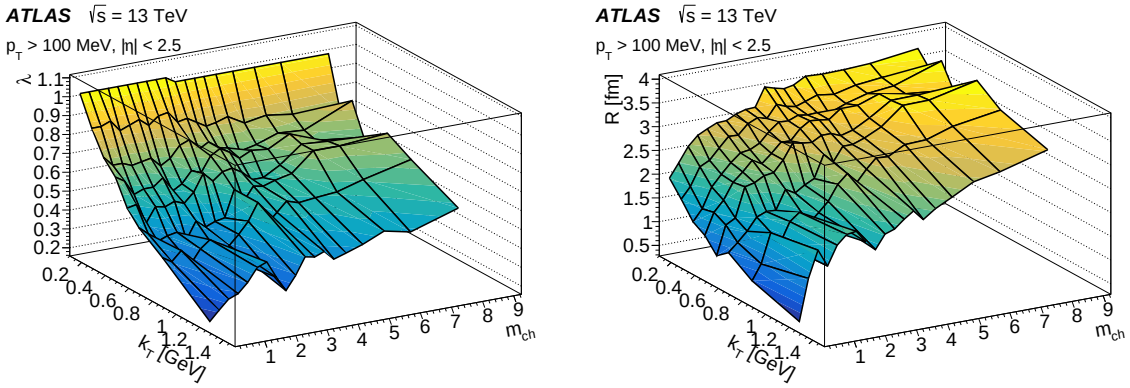

Figure 3: The two-dimensional dependence on m_{ch} and k_T for $p_T > 100$ MeV for the correlation strength, λ (left), and the source radius, R (right), obtained from the fit to the $R_2(Q)$ correlation functions by Eq. 1 using the MB sample for $m_{ch} \leq 3.08$ and the HMT sample for $m_{ch} > 3.08$ [3].

One can see, that the parameter λ decreases monotonically with k_T in all m_{ch} intervals, similar to the behavior seen in Figure 2. The variation of λ with m_{ch} is rather flat for $k_T \lesssim 500$ MeV, which is seemingly contradictory with the clear decrease of λ as a function of m_{ch} seen in Figure 1 for $p_T > 100$ MeV. This arises because particle p_T and hence k_T of the pair increase with m_{ch}, but λ decreases as k_T increases. The overall decrease of λ with m_{ch} when integrated over all k_T is therefore caused rather by the dependence on k_T which is much stronger than the dependence on m_{ch}. The variation of λ with m_{ch} for $k_T > 500$ MeV indicates a slight rise with m_{ch} similar to what is seen in Figure 1 for $p_T > 500$ MeV.

The parameter R also decreases monotonically with k_T in all m_{ch} intervals, with the decrease being more pronounced in lower m_{ch} intervals. A similar decrease is seen in Figure 2. R increases with m_{ch} in all k_T intervals, starting from a lower value at larger k_T. This increase of R flattens off to a plateau level in all k_T intervals. This is similar to the plateau seen in Figure 1. Within the precision of the present data, the onset of the plateau occurs at $m_{ch} \sim 3$ in all k_T intervals.

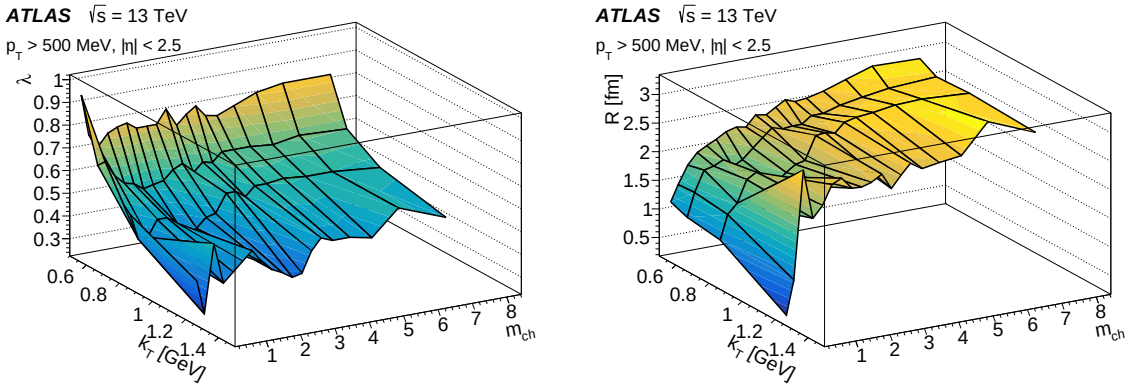

Figure 4: The two-dimensional dependence on m_{ch} and k_T for $p_T > 500$ MeV for the correlation strength, λ (left), and the source radius, R (right), obtained from the fit to the $R_2(Q)$ correlation functions by Eq. 1 using the MB sample for $m_{ch} \leq 3.08$ and the HMT sample for $m_{ch} > 3.08$ [3].

The 2D dependencies for the $p_{\mathrm{T}} > 500$ MeV are shown in Figure 4. The main features are similar to those observed in Figure 3. In particular, the value of R tends to a plateau at large $\mathrm{m_{ch}}$ in all k_{T} intervals, but the plateau level is systematically lower than for $p_{\mathrm{T}} > 100$ MeV, in line with what is observed in Figure 1.

6. Conclusions

Measurements of two-particle BEC of like-charge hadrons with track p_{T}-thresholds of 100 MeV and 500 MeV and $|\eta| < 2.5$ produced in pp collisions at $\sqrt{s} = 13$ TeV recorded by the ATLAS detector at the CERN LHC are presented. The study is carried out using data collected with the MB and HMT triggers. The integrated luminosities are 151 $\mu\mathrm{b}^{-1}$ and 8.4 nb^{-1} for the MB and HMT data samples, respectively. The studies are performed using the $R_2(Q)$ correlation function with unlike-sign particle pairs reference sample fitted by the function predicted by the plane wave approach model applying Cauchy-Lorentz source emission probability distribution. The BEC parameters, R and λ, are studied as functions of a scaled charged-particle multiplicity $\mathrm{m_{ch}}$, the pair average transverse momentum (k_{T}) and in ($\mathrm{m_{ch}}$, k_{T})-intervals.

Source radius parameter R increases linearly with $\sqrt[3]{\mathrm{m_{ch}}}$ up to $\mathrm{m_{ch}} \lesssim 1.7$ (corresponding to $\mathrm{n_{ch}} \lesssim 56$ for $p_{\mathrm{T}} > 100$ MeV) which indicates that the hadronization volume is proportional to the number of produced particles. For high multiplicity ($\mathrm{n_{ch}} \gtrsim 100$ for $p_{\mathrm{T}} > 100$ MeV), the BEC radius R is found to be independent of the charged-particle multiplicity. It confirms previous observation of a high-multiplicity plateau by ATLAS at $\sqrt{s} = 7$ TeV. In addition, in this analysis it is for the first time observed, that this saturation occurs independently of pair k_{T}. The values of saturation of R are: $3.35^{+0.20}_{-0.09}$ fm ($p_{\mathrm{T}} > 100$ MeV) and $2.78^{+0.23}_{-0.09}$ fm ($p_{\mathrm{T}} > 500$ MeV). The double-differential dependencies of fit parameters R and λ are all monotonic. Within the uncertainties of this analysis, the saturation of R occurs at the same value of $\mathrm{m_{ch}}$ in all k_{T} intervals and for both p_{T} thresholds.

Acknowledgments

This work was supported by Ministry of Education, Science, Research and Sport of Slovakia.

References

[1] R. Hanbury Brown and R. Q. Twiss, Phil. Mag. Ser. 7 **45** (1954) 663.

[2] G. I. Kopylov and M. I. Podgoretsky, Sov. J. Nucl. Phys. **15** (1972) 219.

[3] ATLAS Collaboration, Eur. Phys. J. C **82** (2022) 608, arXiv:2202.02218 [hep-ex].

[4] ATLAS Collaboration, JINST **3** (2008) S08003.

[5] ATLAS Collaboration, Eur. Phys. J. C **75** (2015) 466, arXiv: 1502.07947 [hep-ex].

[6] ATLAS Collaboration, Phys. Lett. B **758** (2016) 67, arXiv: 1602.01633 [hep-ex].

[7] ATLAS Collaboration, Phys. Rev. Lett. **116** (2016) 172301, arXiv: 1509.04776 [hep-ex].

[8] M. Deutschmann et al., Nucl. Phys. B **204** (1982) 333.

[9] CMS Collaboration, JHEP **03** (2020) 014, arXiv: 1910.08815 [hep-ex].

[10] ATLAS Collaboration, Eur. Phys. J. C **76** (2016) 502, arXiv: 1606.01133 [hep-ex].